INTERNATIONAL JOURNAL OF
Minerals, Metallurgy and Materials

Volume 32, Number 5, May 2025
Page 1008

Review https://doi.org/10.1007/s12613-025-3090-1

Liquid metal composites: Recent advances and applications

Chunghyeon Choi[1)], *Liyang Liu*[2,3)], *and Byungil Hwang*[4),✉]

1) Department of Intelligent Semiconductor Engineering, Chung-Ang University, Seoul 06974, Rep. of Korea
2) Department of Chemistry and Chemical Engineering, Chalmers University of Technology, Gothenburg SE-412 96, Sweden
3) Wallenberg Wood Science Center, Chalmers University of Technology, Gothenburg SE-412 96, Sweden
4) School of Integrative Engineering, Chung-Ang University, Seoul 06974, Rep. of Korea
(Received: 28 September 2024; revised: 20 December 2024; accepted: 9 January 2025)

Abstract: Liquid metals (LMs), because of their ability to remain in a liquid state at room temperature, render them highly versatile for applications in electronics, energy storage, medicine, and robotics. Among various LMs, Ga-based LMs exhibit minimal cytotoxicity, low viscosity, high thermal and electrical conductivities, and excellent wettability. Therefore, Ga-based LM composites (LMCs) have emerged as a recent research focus. Recent advancements have focused on novel fabrication techniques and applications spanning energy storage, flexible electronics, and biomedical devices. Particularly noteworthy are the developments in wearable sensors and electronic skins, which hold promise for healthcare monitoring and human–machine interfaces. Despite their potential, challenges, such as oxidative susceptibility and biocompatibility, remain. Creating bio-based LMC materials is a promising approach to address these issues while exploring new avenues to optimize LMC performance and broaden its application domains. This review provides a concise overview of the recent trends in LMC research, highlights their transformative impacts, and outlines key directions for future investigation and development.

Keywords: composites; liquid metal; polymer; applications; alloys

1. Introduction

Recently, liquid metals (LMs) have attracted considerable interest [1–2]. Unlike most metals, which are solid at room temperature, LMs remain in a liquid state even at ambient temperatures [3–6]. This unique property makes LMs highly versatile and useful for a wide range of applications, ranging from electronics and energy storage to medicine and robotics [7–9]. LMs typically refer to alloys composed of various metallic elements, such as Ga, In, and Sn [10]. These metals possess several distinctive properties that distinguish them from other materials, including low viscosity [11], high thermal and electrical conductivities [12–13], and excellent wettability [14]. In addition, unlike the well-known LM mercury, Ga-based LMs exhibit minimal cytotoxicity [15] and show enormous potential for use in the biomedical field. Owing to these unique characteristics, LMs are gaining popularity across various industries, and new ways are continuously being explored to harness their potential. The possibilities of LMs, ranging from self-healing materials to flexible electronics, are vast and exciting.

LM composites (LMCs) have recently received considerable attention because of their unique properties and diverse applications [16–21]. Fig. 1 presents an overview of LMCs, categorizing them into their key properties, fabrication methods, and applications [21–29]. LMCs consist of an LM matrix typically composed of Ga or its alloys embedded with various types of particles or fibers. Additionally, some LMCs include a polymer or elastomer matrix that encapsulates the LM, depending on the specific application and design. These composites exhibit enhanced mechanical, thermal, and electrical properties, making them promising candidates for applications in energy storage, flexible electronics, and biomedical devices [30–33]. Initially, LMs were primarily used in filler form to overcome limitations in conductivity and mechanical properties. Early studies demonstrated that incorporating gallium-based alloys, such as eutectic gallium–indium (EGaIn), into various media, such as polymer matrices and carbon-based materials, enhanced their electrical and thermal conductivities while maintaining their intrinsic properties [34–36]. Building on these foundational works, LMCs have evolved to include diverse structures such as LM core–shell composites, LM–polymer composites (LMPCs), and LM–particle composites. Recent trends in LMC research have focused on developing new fabrication methods, exploring novel compositions and forms of embedded materials, and investigating the mechanisms underlying their properties [37–40].

This review discusses the recent research trends in LMCs. It provides a detailed analysis of the unique properties of LMs and examines different types of LMCs and their distinctions. This study also analyzes recent research trends in

✉ Corresponding author: Byungil Hwang E-mail: bihwang@cau.ac.kr
© The Author(s) 2025

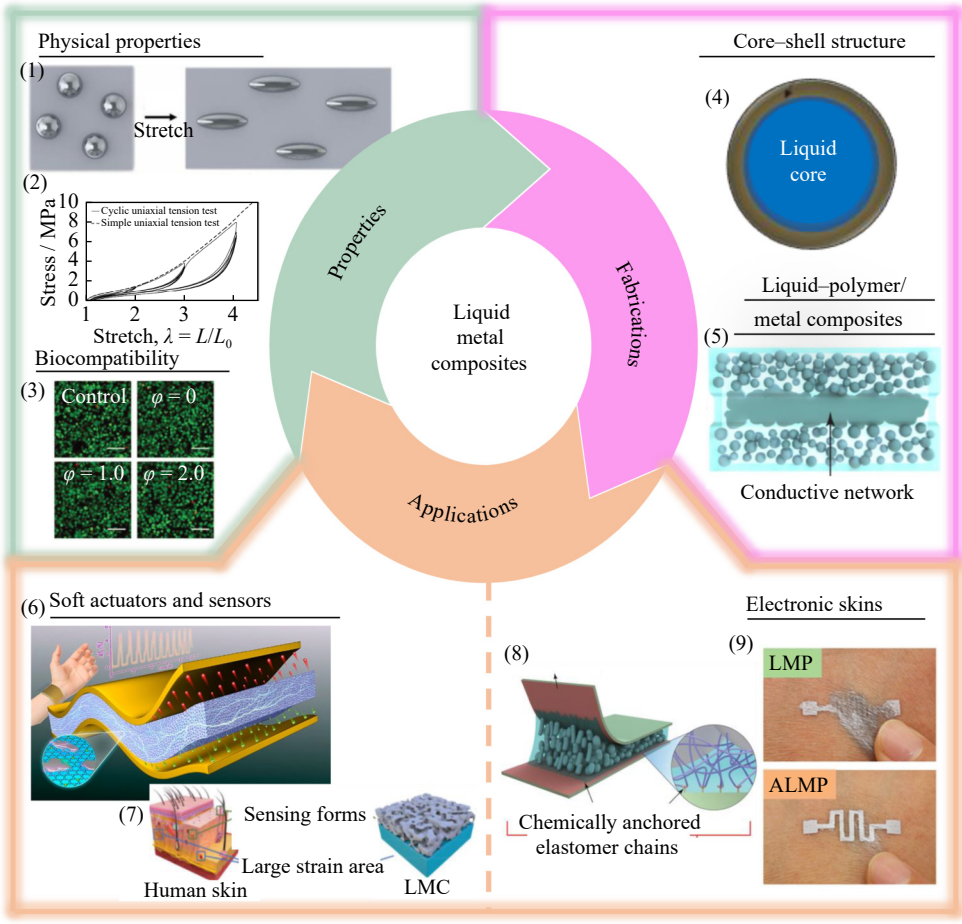


Fig. 1. An overview of LMCs over the five years (φ represents doping ratio; LMP and ALMP represent LM particle and adhesive LM particle, respectively) [21–29]. (1) Reprinted from Ref. [22]. (2) Reprinted from *Eur. Polym. J.*, Vol. 45, J. Diani, B. Fayolle, and P. Gilormini, A review on the Mullins effect, 601-612, Copyright 2009, with permission from Elsevier [23]. (3) X.L. Wang, W.H. Yao, R. Guo, *et al.*, *Adv. Healthcare Mater.*, vol. 7, 1800318 (2018) [24]. Copyright Wiley-VCH Verlag GmbH & Co. KGaA. Reproduced with permission. (4) Reprinted from *Compos. Sci. Technol.*, Vol. 208, C. Chiew and M.H. Malakooti, A double inclusion model for liquid metal polymer composites, 108752, Copyright 2021, with permission from Elsevier [21]. (5) Reprinted form Ref. [25]. (6) Reprinted with permission from Y. Li, Y.G. Cui, M.J. Zhang, *et al.*, *Nano Lett.*, vol. 22, 2817-2825, (2022) [26]. Copyright 2022 American Chemical Society. (7) J.Y. Yang, K.Y. Kwon, S. Kanetkar, *et al.*, *Adv. Mater. Technol.*, vol. 7, 2101074 (2022) [27]. Copyright Wiley-VCH Verlag GmbH & Co. KGaA. Reproduced with permission. (8) Reprinted from Ref. [28]. (9) Reprinted with permission from L. Ding, C. Hang, S.J. Yang, *et al.*, *Nano Lett.*, vol. 22, 4482-4490 (2022) [29]. Copyright 2022 American Chemical Society.

LMCs that are applicable to wearable sensors and electronic skins (e-skins), which are areas of particularly active research. Finally, it presents the limitations of LMCs that require further study and suggests future research directions.

2. Unique properties of LMCs

2.1. Thermal conductivity

Soft materials generally exhibit poor thermal transport properties owing to the dynamics of phonon transport, demonstrating that a decrease in the elastic modulus leads to a reduction in thermal conductivity [41–43]. This explains the thermomechanical trade-off problem faced by materials used in wearable electronic devices. The ultimate goal of developing wearable devices is to achieve both high thermal conductivity and low mechanical stiffness [44]. The incorporation of LMs into polymer matrices addresses these issues. The deformation of LMCs creates thermal conduction pathways, thereby enhancing the thermal transport properties of the material.

Thermal conductivity is estimated according to the Wiedemann–Franz law (Eq. (1)) [45], where κ, σ, L, and T represent the thermal conductivity, electrical conductivity, Lorenz number ($L = 2.44 \times 10^{-8}$ W·S^{-1}·K^{-2}), and absolute temperature, respectively:

$$\frac{\kappa}{\sigma} = LT \tag{1}$$

From this equation, we can infer that the thermal conductivity of LM-embedded elastomers is primarily determined by electronic factors rather than by phonon transport. For EGaIn, the total thermal conductivity is 26.4 W/(m·K) [46–47].

Bartlett *et al.* [22] fabricated an LM-embedded elastomer composed of elongated LM microdroplets (Fig. 2). Their synthesized composite exhibited a high thermal conductivity of (4.7 ± 0.2) W/(m·K) without stress and (9.8 ± 0.8)

W/(m·K) under 400% strain, demonstrating that deformation created thermal conduction pathways within the composite. This enhancement in thermal conductivity is attributed to the thermomechanical coupling effect, in which LM droplets extend into anisotropic microstructures under stress, forming thermal conduction pathways. The study also observed the 10% modulus (Fig. 2(c)) and the induced plastic deformation as functions of the number of cycles (Fig. 2(d)). The 10% modulus represents the stiffness of the material under 10% strain, indicating its resistance to deformation within this range. The modulus decreases slightly, and the plastic deformation slightly increases with the number of cycles. The slight increase in thermal conductivity κ_y could be attributed to the Mullins effect and the permanently increasing aspect ratio of LM particles (LMPs) [23,48]. The study concluded that the incorporation of EGaIn droplets improved the thermal conductivity of the composite without degrading its original mechanical properties (Fig. 2(b)).

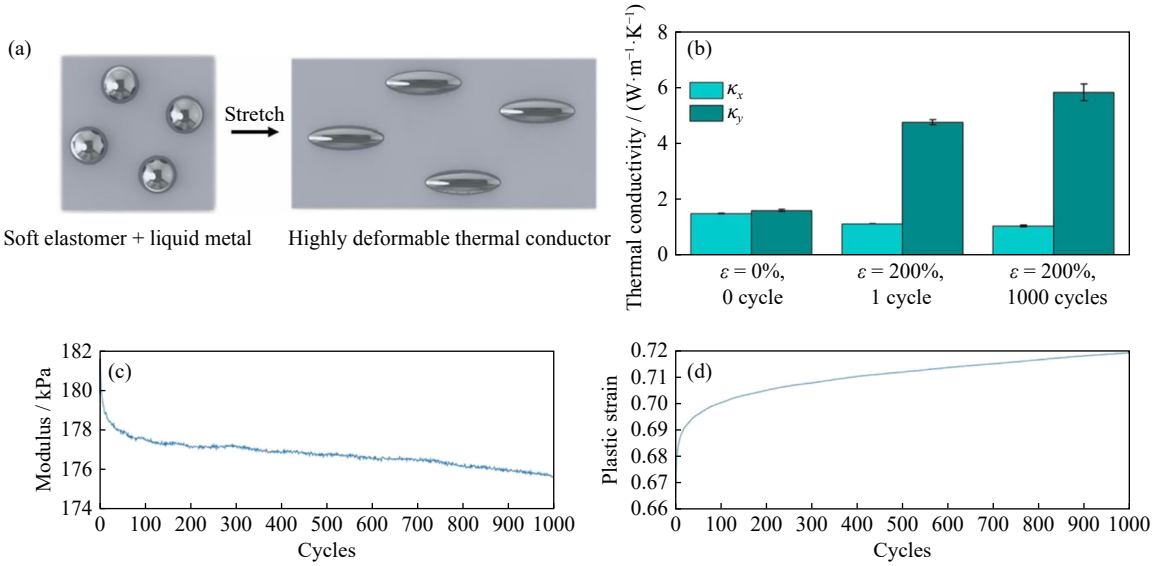


Fig. 2. (a) Schematic illustration of LM-embedded elastomer composites where LM microdroplets are dispersed in an elastomer matrix and, upon deformation, the LM inclusions and elastomer elongate in the direction of stretching. (b) Thermal conductivity of a composite with LM volume fraction (ϕ) = 50% under a strain (ε) of 0%, after stretching to 200%, and following 1000 cycles at 200% (the number of tested samples (n) = 5, error bars represent ±1 standard deviation). (c) The 10% modulus and (d) the induced plastic deformation as functions of the number of cycles. Reprinted from Ref. [22].

2.2. Mechanical property

Fluidic LMs often enhance the structural and functional properties of polymer matrices [49–50]. Incorporating an LM into an elastomer matrix supports the reversible deformability of the composite material because the fluidic characteristics of the LM conform to the direction of deformation and can return to its initial state upon release. Additionally, unlike rigid conductive fillers, LMCs minimize issues related to the aggregation of solid filler particles, such as stress relaxation problems, which are negligible and are known as the Mullins effect. The Mullins effect indicates that elastomers become softer during the first few cycles of deformation (Fig. 3(a)) [23]. Furthermore, an increase in the size of the LM droplets leads to a reduction in the elastic modulus of the composite material, signifying the softening of the material (Fig. 3(b)) [1]. It has also been observed that as the droplet size decreases, the tensile strength of the composite increases.

2.3. Biocompatibility and toxicity

Hg is one of the most well-known types of LMs, leading to the perception that other types, such as Ga- and Bi-based LMs, also possess high toxicity [51]. The toxicity of Hg arises from its high vapor pressure (0.002-mm Hg at 25°C), which allows Hg vapor to be produced and inhaled into the human body through the respiratory system. In contrast, Ga, Bi, and their alloys have negligible vapor pressures under ambient conditions [52]. This means that Ga- and Bi-based LMs do not evaporate easily and thus have lower toxicity with respect to respiratory exposure.

However, the form in which the LM exists can alter its toxicity. Owing to their soft and metallic nature, LMs can be easily transformed into nanoparticles or ions. For instance, the release of In ions from Ga-based alloys causes cytotoxicity only after synthesis [15]. However, further experiments on human cells showed high survival rates, confirming their low toxicity. Nonetheless, Chen *et al.* [53] suggested caution in situations where a large number of ions were generated.

Numerous studies have indicated that bulk-sized nonionic Ga has good biocompatibility and low toxicity [53–54]. However, the size of the LM affects its toxicity because nanoparticles have different toxicological mechanisms compared to bulk metals. Nanosized LMs can be more hazardous as they can be easily transported to organs through the bloodstream. Conversely, Liu *et al.* [54] evaluated the *in vivo* toxicity of LM nanoparticles using drug delivery methods and found no considerable toxicity. In conclusion, recent research has indicated that Ga- and Bi-based LMs possess good biocompatibility. However, the potential toxicity of the LMs

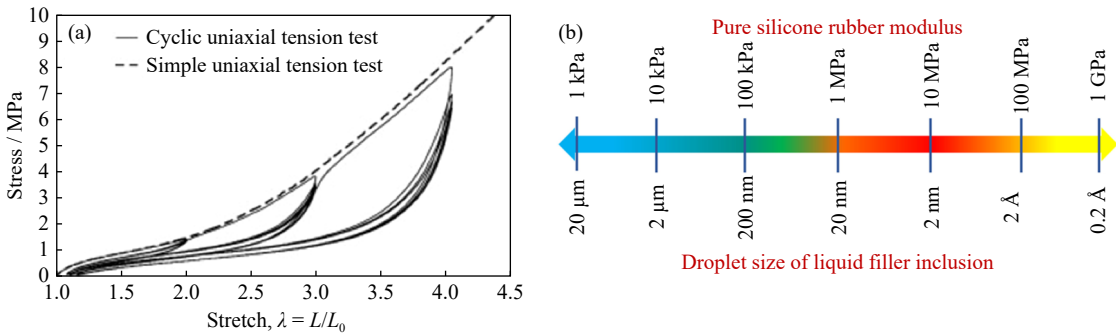


Fig. 3. (a) Stress–strain responses of a 50-phr carbon black-filled styrene butadiene rubber (SBR) undergoing a simple uniaxial tension and a cyclic uniaxial tension with increasing maximum stretch every 5 cycles [23]. (b) Effect of LM inclusion droplet size on the modulus of a silicone elastomer composite [50]. (a) Reprinted from *Eur. Polym. J.*, Vol. 45, J. Diani, B. Fayolle, and P. Gilormini, A review on the Mullins effect, 601-612, Copyright 2009, with permission from Elsevier. (b) Reprinted from *Adv. Colloid Interface Sci.*, Vol. 308, P.S. Banerjee, D.K. Rana, and S.S. Banerjee, Influence of microstructural alterations of liquid metal and its interfacial interactions with rubber on multifunctional properties of soft composite materials, 102752, Copyright 2022, with permission from Elsevier.

must be carefully considered and tested under specific conditions.

The toxicological properties of LMCs differ from those of pure LMs due to the potential influence of additional components that are present in the composites. Although the interaction between LMs and other substances can affect toxicology, recent studies have confirmed that fabricated LMCs demonstrate excellent biocompatibility, supporting their application in the biomedical industry [24,55]. For example, Wang *et al.* [24] conducted a study on the cytotoxicity of LM–Mg particles (Fig. 4(a)). To determine how the concentration of ions derived from the LM affects cytotoxicity, they experimented on a C8161 cell culture medium. After a 48-h reaction, the maximum Mg content was 236.02 mg·L^{-1} (Fig. 4(b)), which falls within the range of biocompatibility. Fig. 4(c) shows that there is almost no cell death. The C8161 cells maintained nearly 100% viability even when in contact with the LM–Mg particles (Fig. 4(d)). The toxicity of the LMPs on other cells demonstrated excellent biocompatibility.

3. Types of LMCs

According to the original definition, composite refers to a new type of material system in which two or more different materials are combined in a specific manner. By mixing different materials, each material can exhibit its advantages and create a synergistic effect. LMCs also exhibit enhanced performance when mixed with other fillers. By adding various fillers to an LM matrix, the benefits of LMs can be maximized while their drawbacks can be mitigated. Generally, LMCs can be categorized into three groups: LM core–shell composites, LMPCs, and LM–particle composites. Recently, technological trends in LMCs have included combining two or more categories to synthesize optimized composites.

3.1. LM core–shell composites

LM core–shell composites are nanosized ordered assembly structures in which the LM forms the core, and other materials are chemically bonded and coated on the surface of the LM. This unique core–shell structure integrates the different properties of the material's interior and exterior, thereby complementing each other's deficiencies [56–59]. LM core–shell composites can be divided into naturally occurring and artificially prepared core–shell composites. When the surface of the LM comes into contact with air, naturally occurring core–shell composites form, creating a thin metal oxide layer around the LM core. The thin oxide layer formed on the surface of the LM creates a strong physical structure and exhibits a thickness of approximately 0.7–3.0 nm under vacuum conditions [60]. When exposed to ambient oxygen, it forms almost instantaneously on the LM surface [61]. Artificially manufactured core–shell composites are fabricated by integrating different types of materials to enhance various properties of LMCs, including elasticity, surface tension, and catalytic functionality [59].

There are three main methods for synthesizing LM core–shell composites: surface oxidation, ligand assembly, and galvanic replacement (Fig. 5). Surface oxidation occurs when the LM is exposed to an oxidizing environment. A thin oxide shell forms almost instantaneously around the LM, preventing the bulk LM from fragmenting or dispersing into smaller particles [62]. The ligand assembly method is often used for the stabilization and functionalization of metallic substances. When applied to LMs, ligand assemblies compete with surface oxidation, minimizing the formation of the oxide skin. Ligands include sulfhydryl compounds [63], polyphenols [64], silanes [65], polymers [66], and proteins [67]. Galvanic replacement is an electrochemical process in which one metal is oxidized by the ions of another metal with a higher reduction potential. For LMs such as Ga, In, and Sn, which have low standard reduction potentials, galvanic replacement can be performed using elements with higher reduction potentials, such as Au and Ag [54]. Galvanic replacement is used to enhance the stability and modulate the thermal/electrical conductivity of core–shell composites.

Sonochemical synthesis uses ultrasound to induce physicochemical reactions and transformations to produce liquid metal particles (Fig. 5). Sonochemical synthesis involves

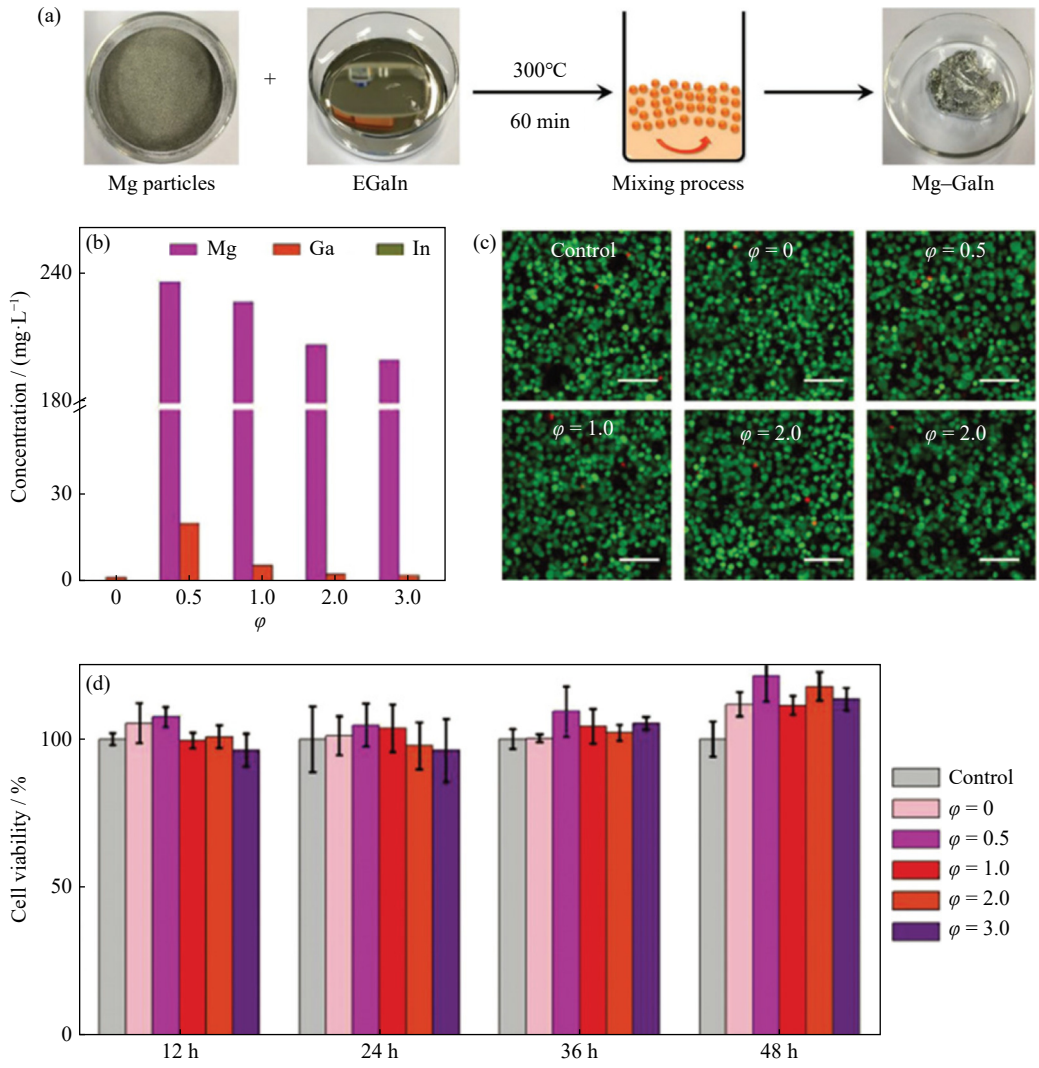


Fig. 4. Toxicological testing of LM–particle composites: (a) preparation process for LM–Mg composites; (b) metal ion concentration of a C8161 cell culture medium soaked in Mg–GaIn composites after 48 h of immersion time; (c) survival of C8161 cells after 48 h of culture with the cell culture medium referred to in (b). Scale bars, 100 μm. (d) Test of C8161 cell viability after 12, 24, 36, and 48 h of reaction in the cell culture medium immersed in Mg–GaIn composites. X.L. Wang, W.H. Yao, R. Guo, *et al.*, *Adv. Healthcare Mater.*, vol. 7, 1800318 (2018) [24]. Copyright Wiley-VCH Verlag GmbH & Co. KGaA. Reproduced with permission.

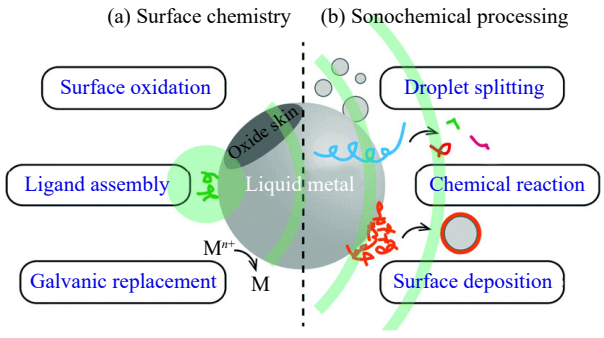


Fig. 5. Overview of core–shell liquid metal particles, including (a) their surface chemistry and (b) fabrication. Reproduced from Ref. [54] with permission from the Royal Society of Chemistry.

three main processes: droplet splitting, chemical reactions, and surface deposition [68–70]. In the case of LMs, large volumes are fragmented into smaller droplets through mechanical agitation and C–C bond breakage during sonochemical synthesis. For polymers, sonochemical synthesis involves fragmentation via C–C bond cleavage during the chemical reactions. During ultrasonic treatment (surface deposition), all reactants, including solvent/ligand molecules and ions, are attached to the surface of the LM. This is because the LM splits into droplets, increasing the surface area and providing opportunities for other reactants to precipitate.

Zhao *et al.* [71] reported the growth of core–shell nanohybrids using LM nanodroplets through a galvanic replacement reaction within an LM emulsion system (Fig. 6(a)). By employing Ga–Zn as the core component, they completed the core–shell structure with shells composed of single metals, such as Ag, Ni, Cu, Co, and Fe, or bimetallic components, like CoNi, AgNi, CuNi, AgCo, and CuCo. The pristine-oxide skin of the LM was removed by the shear force generated during sonication, exposing an oxide-free surface with high surface energy and separating LM droplets from the bulk substrate. When these separated droplets encountered metal ions with a reduction potential higher than Ga/Ga^{3+}, a galvan-

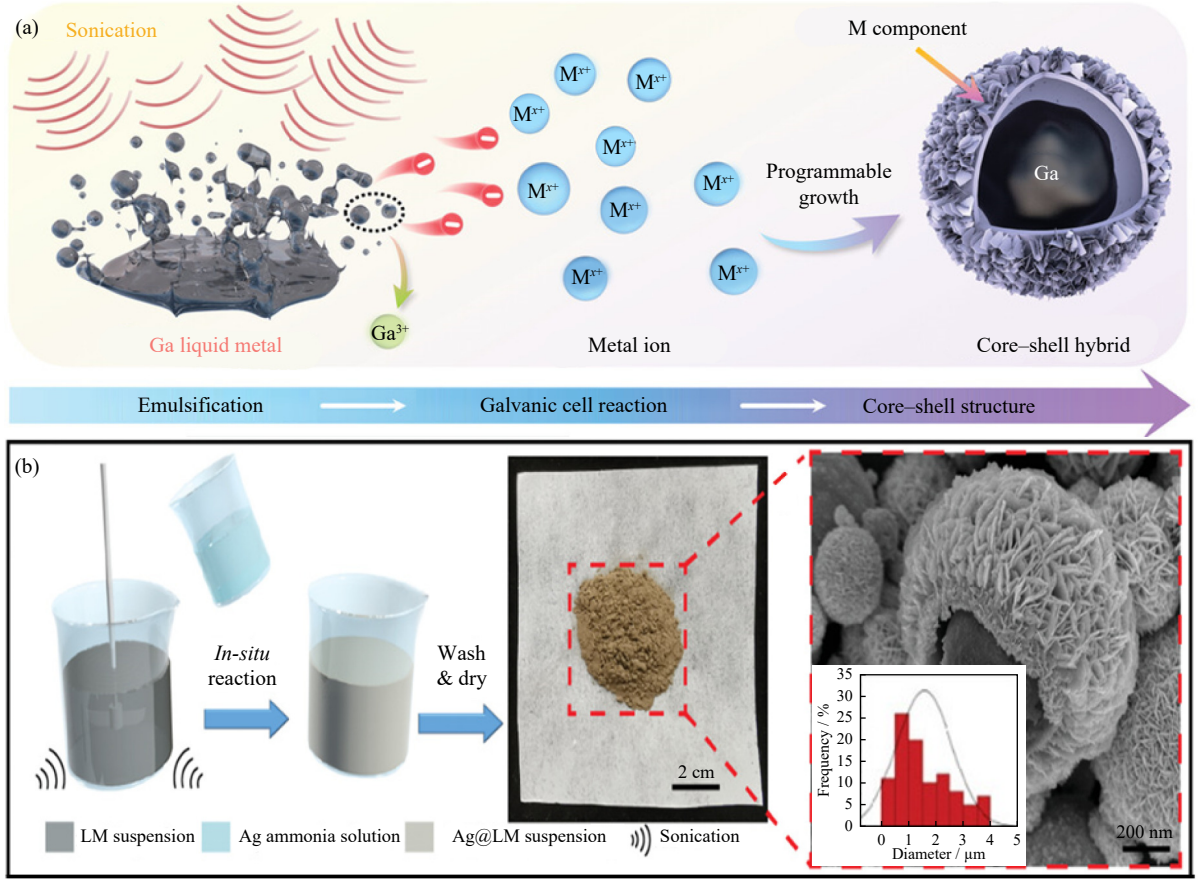


Fig. 6. (a) Fabrication process: The LM is emulsified using sonication shear force in a metal solution, enabling a galvanic replacement reaction between LM droplets and metallic cations. (b) Schematic illustration of the fabrication process for Ag@LMPs with corresponding digital photos, along with an scanning electron microscope (SEM) image of Ag@LMPs and the inset showing the diameter distribution. (a) B. Zhao, Y.Q. Du, H.L. Lv, *et al.*, *Adv. Funct. Mater.*, vol. 33, 2302172 (2023) [71]. Copyright Wiley-VCH Verlag GmbH & Co. KGaA. Reproduced with permission. (b) R.M. Zheng, Z.F. Peng, Y. Fu, *et al.*, *Adv. Funct. Mater.*, vol. 30, 1910524 (2020) [72]. Copyright Wiley-VCH Verlag GmbH & Co. KGaA. Reproduced with permission.

ic replacement reaction occurred, uniformly depositing metal materials onto the droplet surface. This process resulted in the formation of core–shell structures with LM as the core. The core–shell nanohybrids were used as microwave absorbers with unprecedented microwave dissipation abilities. Specifically, the Ga–Ni nanohybrids achieved a minimum reflection loss (RL_{min}) value of −55.9 dB at 7.68 GHz with a thickness of 1.44 mm. They proposed a simple sonication-based method as a scalable approach and demonstrated its potential applicability to other oxides or sulfides using similar strategies.

Zheng *et al.* [72] fabricated core–shell-structured Ag@LMPs by coating the surface of the LM with nanosilver through *in situ* chemical reduction (Fig. 6(b)). The Ag@LMPs exhibited a high conductivity without requiring additional treatments, such as mechanical sintering or the addition of conductive materials. Furthermore, even when a certain stress level caused damage to the materials, the LM within the core flowed out, effectively maintaining the conductive network. The nanosilver coating prevented the corrosion of the LM in acidic or alkaline environments, contributing to its excellent durability. Notably, the material demonstrated outstanding real-time self-repairing capabilities, retaining its initial conductivity even after scratching, highlighting its potential as a next-generation conductive filler.

In a recent study, Wang *et al.* [73] fabricated LM-coated copper microparticles with a core–shell structure. The LM core–shell composite, as shown in Fig. 7(a), was produced by coating the LM with copper, followed by annealing. The resulting composite exhibited excellent microwave absorption and optimal reflection loss. This remarkable performance was due to the unique core–shell structure of the composite material, which enhanced dielectric losses such as dipolar, interfacial, and dielectric polarization. Chiew and Malakooti [21] introduced a double-inclusion model using polymer matrices with core–shell LM droplets, as illustrated in Fig. 7(b). The proposed model demonstrated a more accurate prediction of Young's modulus for LMCs compared to Eshelby's theory while also extending its applicability to estimate permittivity and thermal conductivity. By providing an efficient and flexible design framework for composites with nanoscale and microscale LM inclusions, this model has shown its potential to accelerate the development of advanced composites at a low cost and complexity.

3.2. LMPCs

LMPCs combine LM droplets with polymer materials. Amid the sustained interest in flexible electronics, recent

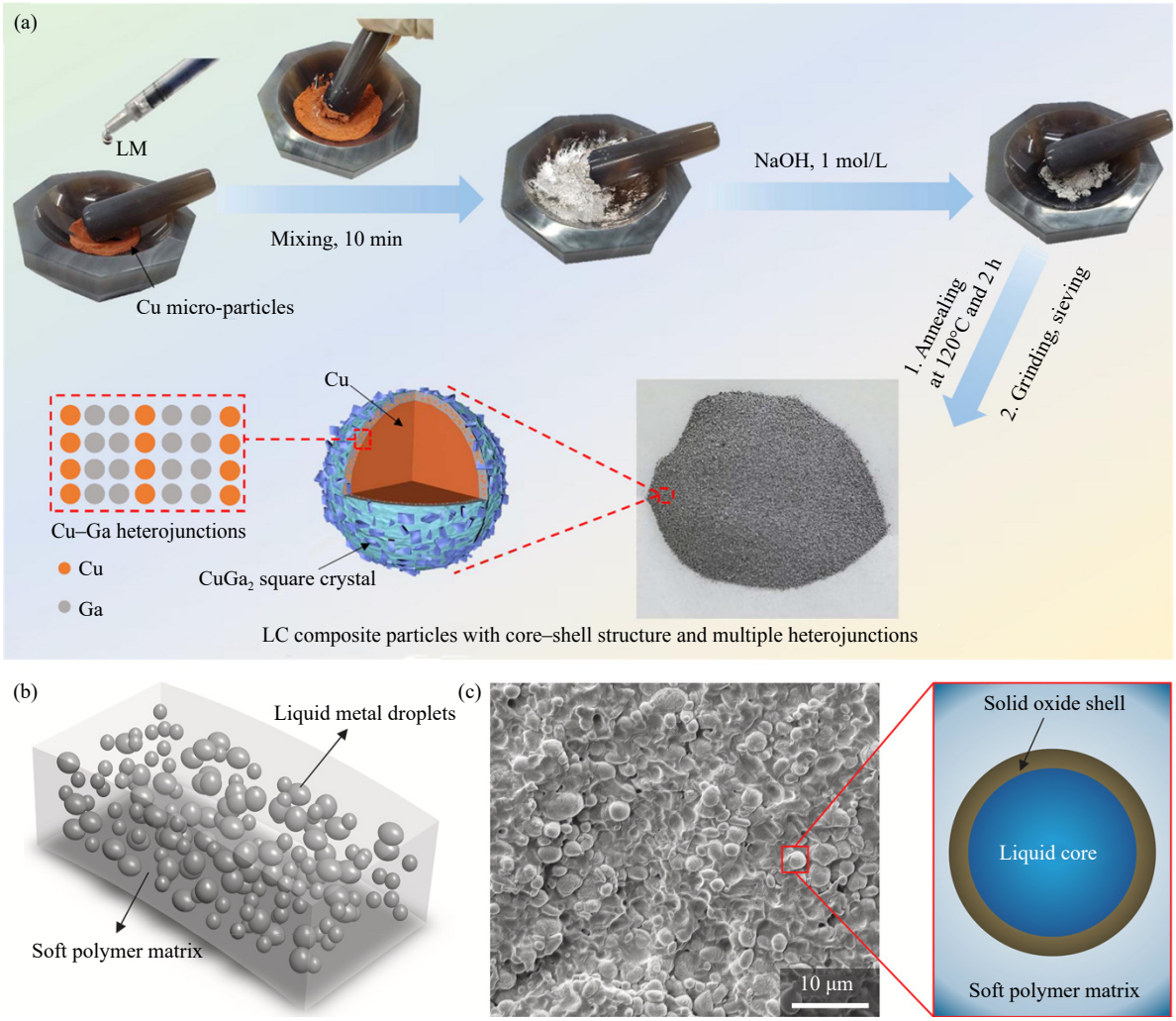


Fig. 7. (a) Schematic illustration of the preparation process for LM–copper (LC) composite microparticles [73]. (b) Schematic of LMPCs; (c) micrograph of the dispersed EGaIn droplets in polydimethylsiloxane (PDMS) (inset: core–shell structure of embedded LM inclusions) [21]. (a) Reprinted from *J. Colloid Interface Sci.*, Vol. 607, Y. Wang, Y.N. Gao, T.N. Yue, X.D. Chen, R.C. Che, and M. Wang, Liquid metal coated copper micro-particles to construct core–shell structure and multiple heterojunctions for high-efficiency microwave absorption, 210-218, Copyright 2022, with permission from Elsevier. (b, c) Reprinted from *Compos. Sci. Technol.*, Vol. 208, C. Chiew and M.H. Malakooti, A double inclusion model for liquid metal polymer composites, 108752, Copyright 2021, with permission from Elsevier.

studies have considerably focused on LMPCs [25,30–33] Solid particles have traditionally been used as conductive fillers in polymer matrices. However, the addition of solid conductive fillers deteriorates the mechanical properties and deformability of composite materials. Therefore, LMs have been introduced as new conductive fillers that maintain mechanical performance during deformation. Additionally, the incorporation of LM fillers enhanced the electrical and thermal conductivities of polymer matrices while maintaining their flexibility.

The three common manufacturing strategies for preparing LM droplets for LMPCs are planetary mixing, overhead mixing, and sonication (Fig. 8). These methods not only enhance the processability of LMs but also increase their compatibility with polymers. Both shear and overhead mixing were sustained in single-pot synthesis. However, considerable variations in particle size limit these synthetic processes [25,30–33] Ultrasonication is necessary for manufacturing LMPCs with minimal particle size variation. Furthermore, utilizing the sonication method on an LM solution containing monomers can promote free-radical polymerization reactions, thereby enhancing the compatibility between the two materials [74]. The synthetic processes for LM–polymer matrices are straightforward, cost-effective, and advantageous for LMPCs.

However, LMPCs are hindered by the weak compatibility between the LM, which becomes semisolidified due to the

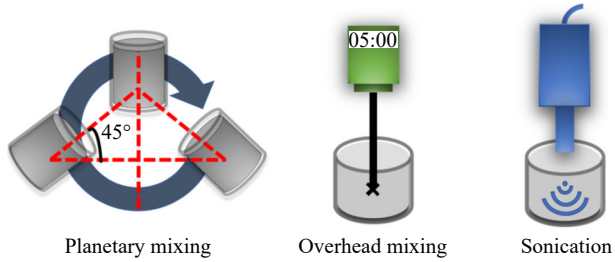


Fig. 8. Schematic of the fabrication strategies for LM droplets.

formation of a surface oxide layer, and polymer matrices. To address this issue, LMs can be dispersed into nanodroplets to enhance their compatibility with polymers. Another issue with LMPCs is their insulating properties. LM droplets within LMPCs are separated by the formed oxide layer. Therefore, the developed LMPCs inherently possess insulation and do require posttreatment. The most effective and straightforward strategy for enhancing the electrical conductivity of composites is mechanical sintering, which involves stretching, compression, and shear friction (Fig. 9(a)) [25]. Mechanical sintering aligns the separated LMs to create conductive paths. This technique involves applying mechanical forces such as stretching, compression, or shear friction, which break the oxide layers on the LM droplets, enabling electrical connectivity. Mechanical sintering considerably enhances the electrical conductivity of LMCs, making it a foundational method for their application in flexible and wearable electronics [75]. Recently, Hajalilou *et al.* [76] developed a sinterless-printed flexible electronic device based on biphasic LMCs (Fig. 9(b)). The manufactured composite consisted of a ternary system of EGaIn, a styrene–isoprene (SIS) thermoplastic elastomer, and conductive filler particles. Experiments revealed that the addition of conductive filler particles created a percolation network, fundamentally rendering the LMPC conductive. However, further research using different filler particles is required to achieve direct electrical conductivity without postprocessing.

Xue *et al.* [77] introduced LM elastomers incorporating elastomer particles to jam and immobilize the LM (Fig. 10). Typically, PDMS or Ecoflex is used as an elastomer to synthesize embedded LM elastomers, which require several hours of thermal curing. During this time, the LMPs embedded within the elastomer matrix settle at the bottom of the composite owing to their density. These precipitated LMPs reduce the dielectric, electrical, and thermal conductivities of the composites. To overcome this issue, the load of the LM can be increased; however, this would eventually increase the composite weight and cost. Moreover, excessive filler loading can lead to metal leaching. The new concept for LMCs is called LM elastomers with PDMS particles (LMEPs). By trapping PDMS particles in the LMEP, the sinking of the LM can be prevented, enhancing the overall properties of the composite.

In particular, in terms of electrical properties, a small amount of LM (10% < volume fraction of LM (ϕ_{LM}) < 30%) within the LMEP inadequately forms conductive pathways, resulting in insulative behavior (Fig. 10(c)). However, the LMEP with ϕ_{LM} = 40% demonstrates conductivity, proving that the volume fraction of the LM is a crucial factor for determining the electrical conductivity of the composite. As shown in Fig. 10(b), the conductive LMEP includes inherent conductive pathways that make the composite conductive

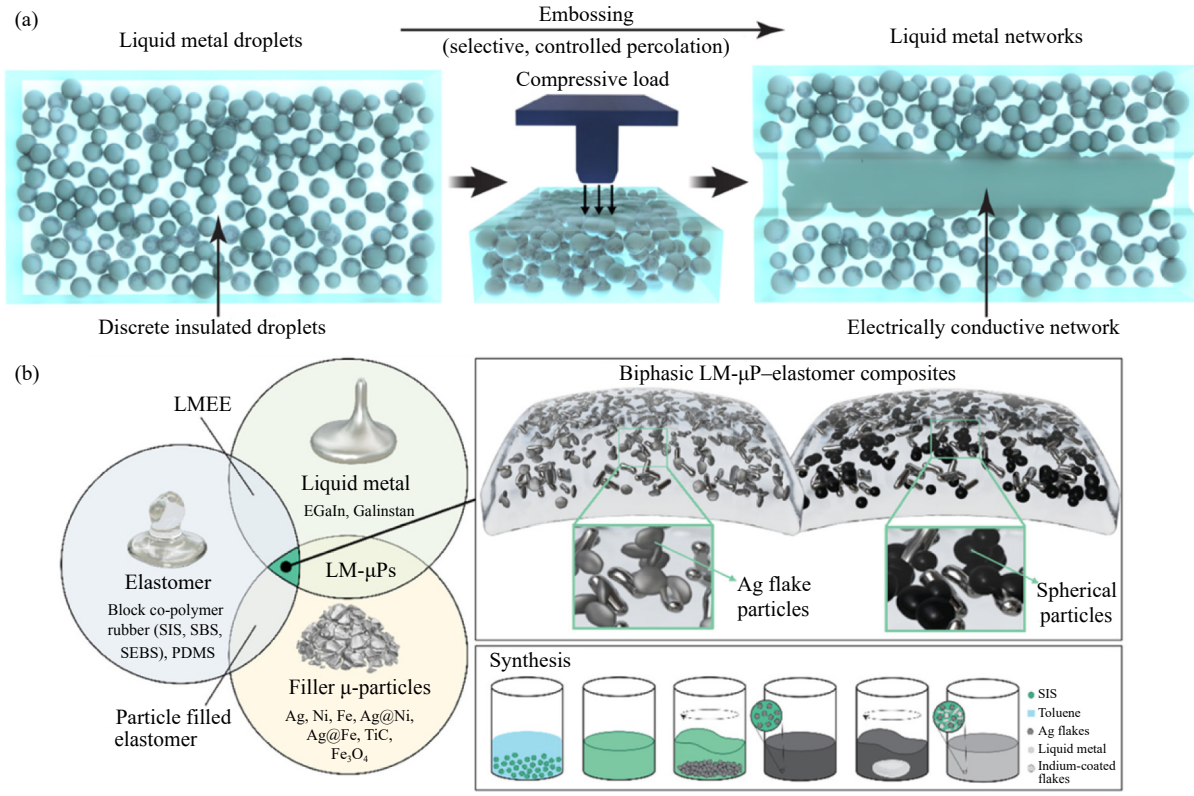


Fig. 9. (a) Schematics illustrating the process of embossing, where discrete insulating droplets of the LM are selectively embossed to form a connected conductive network. (b) LM binary and trinary composites: constitutional materials, synthesis, and characterization performed in this article [76]. The abbreviations in the figure are defined as follows: LMEE (liquid metal embedded elastomer), SBS (styrene-butadiene-styrene), SEBS (styrene-ethylene-butylene-styrene), and μP (microparticles). (a) Reprinted from Ref. [25]. (b) A. Hajalilou, A.F. Silva, P.A. Lopes, E. Parvini, C. Majidi, and M. Tavakoli, *Adv. Mater. Interfaces*, vol. 9, 2101913 (2022) [76]. Copyright Wiley-VCH Verlag GmbH & Co. KGaA. Reproduced with permission.

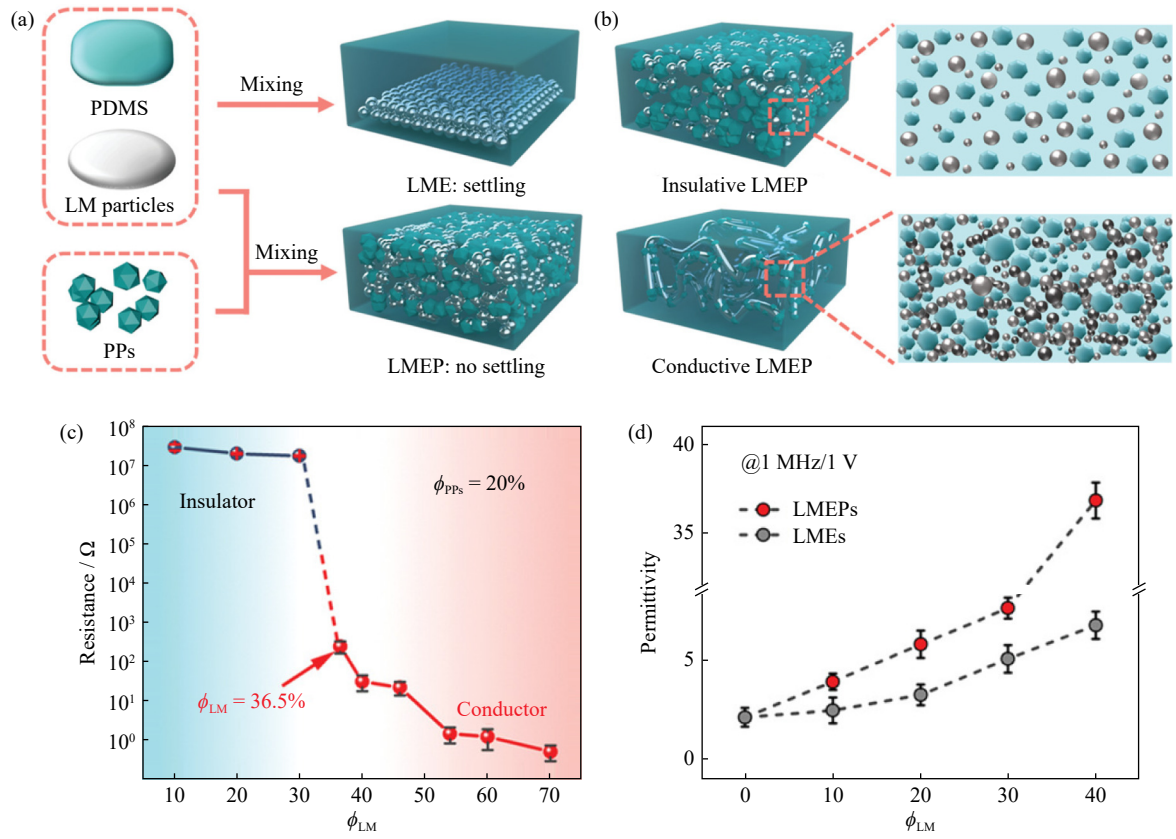


Fig. 10. (a) Schematic of the fabrication processes for the settled liquid metal elastomer (LME) and the LMEP. PPs refers to polydimethylsiloxane particles. (b) Conductive and dielectric characterization of the LMEP: schematics of the insulative LMEP (top) and the conductive LMEP (bottom). (c) Conductive threshold of the LMEP with ϕ_{PPs} = 20%. (d) Plot of permittivity versus ϕ_{LM} of the settled LMEs and the LMEPs. X.T. Xue, D.G. Zhang, Y.L. Wu, *et al.*, *Adv. Funct. Mater.*, vol. 33, 2210553 (2023) [77]. Copyright Wiley-VCH Verlag GmbH & Co. KGaA. Reproduced with permission.

without any sintering process. Fig. 10(d) shows the permittivity plot of the LMEP/LME versus the volume fraction of LM. As seen in Fig. 10(d), the permittivity increases with the ϕ_{LM} value, indicating that the permittivity is closely linked to the dispersion of the LM within the composite. The LMEP shows higher permittivity than the LME, which can be attributed to the well-dispersed LM creating a jamming effect within the composite. At an ϕ_{LM} of 40%, the LMEP exhibits a high permittivity value of approximately 37.7, indicating the formation of conductive paths within the material. The threshold of the LMEP is lower than that of the LME, which reduces the overall density and cost of the composite material. This approach, utilizing various materials such as silicone particles or CNC particles, can enhance the stability of composites and enable the development of new physical properties.

3.3. LM–particle composites

Recently, LM–particle composites have been extensively studied because the addition of particles considerably enhances the overall properties of LMs [78–80]. In this case, the LM serves as the matrix, and the particles are considered additives. To enhance the thermal conductivity of LMs, metal particles doped with a high thermal conductivity are added to the LM matrix. Here, the particles act as a medium for improving thermal conductivity. Preparation during manufacturing requires oxidation-mediated preparation because the formation of an oxide skin can enhance thermal conductivity. The overall characteristics of LM–particle composites can vary depending on the functional properties of the added metal particles. Particles incorporated into the LM are not limited to metals; they can also include nonmetallic materials (e.g., plastic, ceramic, and inorganic salt particles such as copper oxide, silicon oxide, $NaHCO_3$, and carbon nanotubes). While much of the previous research has focused on metal particles to enhance properties such as magnetism, thermal conductivity, and thermodynamic characteristics, these nonmetallic materials offer additional possibilities for tailoring composite properties. The manufacturing strategies for LM–particle composites are similar to those for LMPCs [4,30,81]. Solid-particle fillers are dispersed in the LM and uniformly mixed through planetary mixing, overhead mixing, and sonication. In LM–particle composites, it is crucial for the added particles to retain their inherent properties while being uniformly dispersed within the LM. Therefore, appropriate fabrication strategies are essential.

For example, Kong *et al.* [82] addressed the challenges of pure LMs, such as intermediate thermal conductivity, surface diffusion difficulties, and pump-out issues, by incorporating tungsten (W) microparticles into an LM matrix (Fig. 11). Although LMs often exhibit high thermal conductivities, they are still insufficient when used alone. W, an ideal can-

didate material for enhancing thermal conductivity, was integrated with an LM matrix to achieve optimal thermal conductivity. Moreover, W is chemically inert, which ensures the overall stability of LM–particle composites. Fig. 11(a) and (b) shows the processes conducted in O-deficient environments, while Fig. 11(c) and (d) illustrates the processes performed in O-rich environments, highlighting the role of oxides through different shear mixing procedures to clarify their function.

4. Recent advances in LMC applications

4.1. Soft actuators and sensors

Recent advancements in wearable electronic devices that can adhere to human skin, robotic skin, and biological tissues have attracted considerable attention. Among the various types of wearable devices, flexible strain sensors for monitoring human activity and health have been extensively researched [26–27,83]. The development of high-performance flexible strain sensors requires high sensitivity and reliable responsiveness. Functional nanomaterials and polymers are commonly used for synthesizing strain sensors. However, the weak adhesion between the matrix and sensing materials in these conventional materials often compromises sensing performance and durability. LMCs offer a solution to these challenges because of their high surface energy, which facilitates the restoration of their initial shape and properties after deformation.

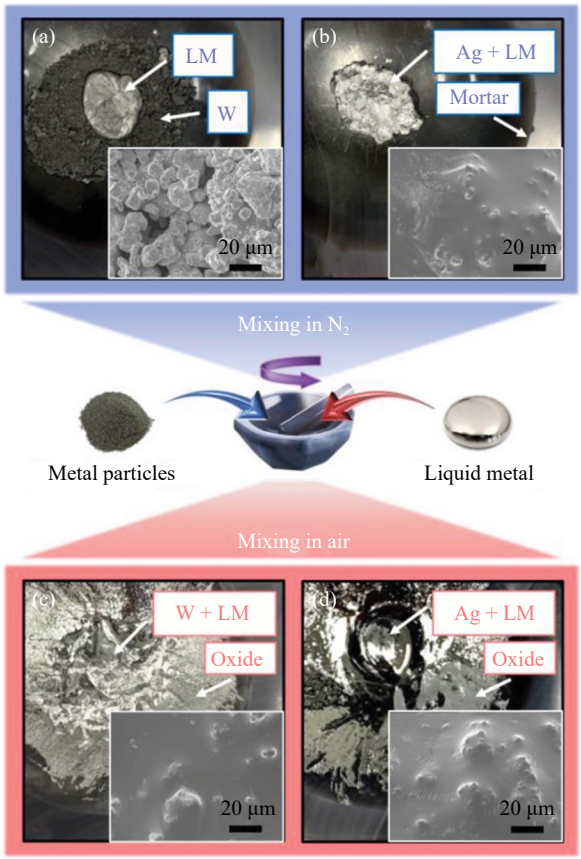


Fig. 11. Schematic illustration of LM–X fabrication. Metal particles are shear-mixed with the LM using a mortar and pestle, and the images show the paste-like morphology of LM–W and LM–Ag in the mortar. (a) W powder and LM mixing in an oxygen-deficient environment demonstrates the non-wetting behavior of W. (b) Ag powder and LM mixing in an oxygen-deficient environment forms a paste with no additional oxide wetting along the mortar. (c) W powder and LM mixing in an oxygen-rich environment leads to paste formation with excess oxides along the mortar. (d) Ag powder and LM blending in an oxygen-rich environment with excess oxide coating the mortar wall. The inset SEM images for the respective mixing conditions show the surface texture of the mixtures. W. Kong, Z.Y. Wang, M. Wang, *et al.*, *Adv. Mater.*, vol. 31, 1904309, (2019) [82]. Copyright Wiley-VCH Verlag GmbH & Co. KGaA. Reproduced with permission.

In their recent study, Li *et al.* [26] developed an ultrasensitive pressure sensor sponge using an LMPC incorporating PDMS, LM, and nitrogen-doped graphene nanosheets (N-GNSs), achieving rapid response/recovery times of 0.41 s/0.12 s and sensitivity up to 477 Pa^{-1}. The introduction of LM helped the composite maintain excellent sensor performance by enabling easy recovery after deformation owing to its high surface energy. Furthermore, their proposed PDMS/LM/GNS sponge sensor exhibited superior response values to PDMS/GNS sponge sensors, thereby enhancing the performance of the pressure sensors (Fig. 12(a)). Yang *et al.* [27] demonstrated the high sensitivity of LMs under small stresses by synthesizing a capacitive strain sensor inspired by the skin using a bilayer LM elastomer-based structure. This bilayer structure consisted of an LM elastomer foam on top and a pure elastomer slab underneath. By integrating these two layers, the pressure sensor can measure large dynamic range stresses with high sensitivity (0.073 kPa^{-1}) (Fig. 12(b) and (c)). Additionally, incorporating LM into the elastomer increased the sensitivity without altering the elastic modulus of the sensor, owing to its high surface energy. However, a critical challenge for these LMPC-based pressure sensors is the risk of metal leakage from the matrix under deformation. Such metal leakage can lead to deterioration of the mechanical properties of the sensor. Therefore, encapsulating LM droplets within an elastomer matrix is crucial. He *et al.* [83] reported a flexible and recyclable LM-embedded elastomer composite encapsulated by a carbonyl iron particle (CIP)/PDMS hybrid matrix to prevent metal leakage. In their recent study, the composite demonstrated stable mechanical and electrical performance under various bending angles and strain rates (Fig. 12(d) and (e)). For instance, increasing the number of LM droplets improved the tensile strength of a composite with a 30wt% CIP. They explained that the addition of LM enhanced the surface tension at the solid–liquid interface, thereby improving the adhesion between the LM droplets and the polymer matrix. These results confirm the mechanical robustness and flexibility of the synthesized LMPCs. The multifunctional characteristics of pressure sensors based on LMCs (high sensitivity, mechanical robustness, flexibility, and rapid response/recovery times) have been applied to various flexible electronic devices for medical monitoring systems.

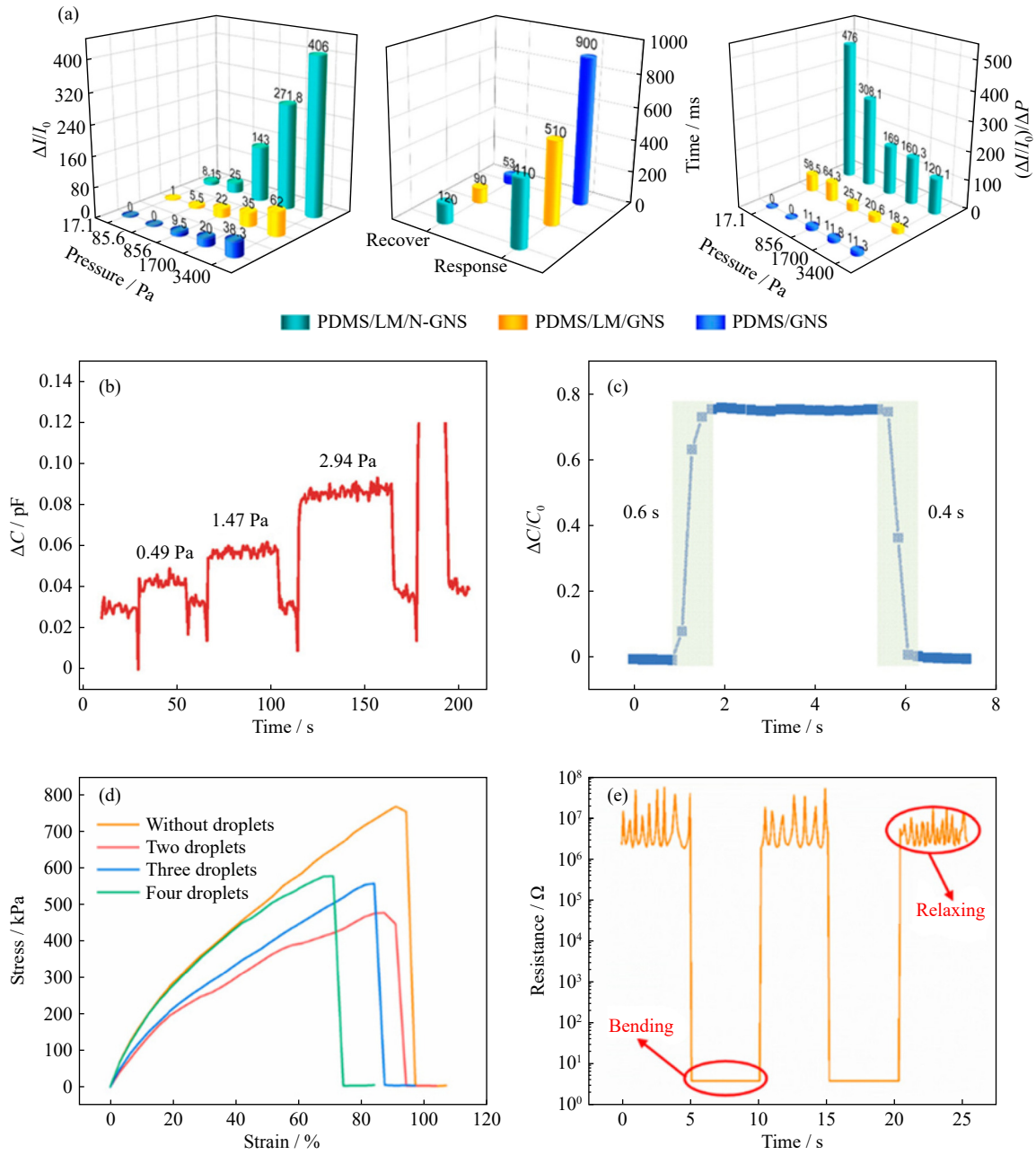


Fig. 12. (a) Comparison of the response values ($\Delta I/I_0$), response/recovery times, and sensitivity of PDMS/GNS, PDMS/LM/GNS, and PDMS/LM/N-GNS sponges. ΔP is the changing pressure. (b) Smallest measurement limit of bilayer of liquid metal elastomer foam (B-LMEF); (c) response time of B-LMEF to touch and release. $\Delta C/C_0$ is the capacitance variation ratio. (d) Stress–strain curves of the unfilled and hybrid liquid metal droplets embedded elastomer (H-LMDE) composites embedded with different numbers of droplets (30wt% CIP content); (e) resistance variation when bending the finger. (a) Reprinted with permission from Y. Li, Y.G. Cui, M.J. Zhang, *et al.*, *Nano Lett.*, vol. 22, 2817-2825, (2022) [26]. Copyright 2022 American Chemical Society. (b, c) J.Y. Yang, K.Y. Kwon, S. Kanetkar, *et al.*, *Adv. Mater. Technol.*, vol. 7, 2101074 (2022) [27]. Copyright Wiley-VCH Verlag GmbH & Co. KGaA. Reproduced with permission. (d, e) Reprinted with permission from X.K. He, J.P. Wu, S.H. Xuan, S.S. Sun, and X.L. Gong, *ACS Appl. Mater. Interfaces*, vol. 14, 9597-9607, (2022) [83]. Copyright 2022 American Chemical Society.

4.2. E-Skins

Recent advancements in soft electronics, including e-skins, have attracted increasing attention, particularly for applications such as medical monitoring and biomedicine [28–29,49,80–81]. The development of high-performance soft electronic devices with excellent durability requires high-performance e-skins that can effectively interface with biological tissues. The key attributes of e-skins include elasticity, self-healing behavior, good adhesion to human skin, and biocompatibility. These composites must be stretchable to accommodate strain induced by movement, possess self-healing capabilities to extend their operational lifetime, adhere well to the human skin, and be minimally cytotoxic for safety purposes. Ga-based LM alloys satisfy these requirements for high-performance e-skins by offering unique physical and chemical properties. These properties stem primarily from the high thermal conductivity of LMs and the spontan-

eous formation of oxide skins around them, which enhance their flexibility and unique characteristics.

In a recent study, Pozarycki *et al.* [28] introduced methods for enhancing the toughness of LM-elastomer composites. Despite the multifunctionality of LM-elastomer composites, their integration into systems composed of diverse materials poses challenges owing to their poor adhesive control. The chemical anchoring methodology proposed by Pozarycki *et al.* improved the adhesion of LMCs to various constituents. This method enables permanent adhesion of LMCs through surface treatment processes using oxygen plasma and organosilane (3-aminopropyl)triethoxysilane (APTES). As shown in Fig. 13(a), the untreated surfaces exhibit reduced adhesive strength compared to the chemically treated surfaces. T-peel tests were conducted to evaluate the adhesion performance, and the manufactured LMCs were adhered between two flexible polyethylene terephthalate (PET) substrates. Fig. 13(b) shows that the untreated samples experienced cohesive failure between the PET surface and the composite, whereas the treated samples showed material failure over interfacial bond failure with the PET surface. Chemical anchoring induces crack propagation in a controlled manner within the composite, thereby increasing the fracture energy. To investigate the profound impact of LM microstructures on fracture energy, LM volume loads with varying LM volume fractions and diameters were prepared. The fracture energy (G_c) decreases with the volume fraction and diameter of the LM, as shown in Fig. 13(c). Decreasing the size of the LM droplets increases the ratio of the external solid surface area to the internal liquid volume, thereby effectively enhancing the stiffness. Consequently, this increased stiffness has the potential to reinforce LMCs. The development

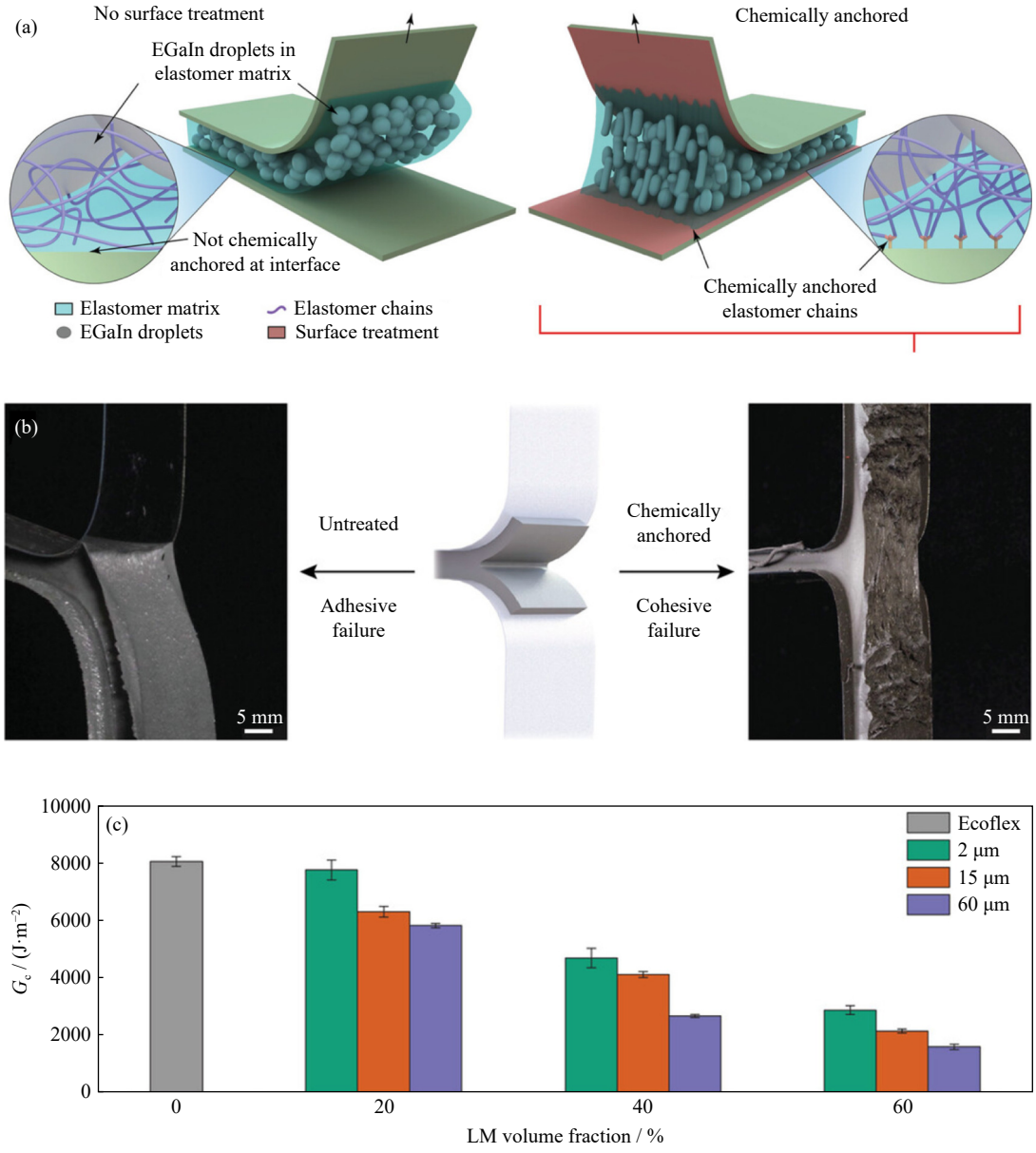


Fig. 13. (a) Schematic representation of LMC adhesion without (left) and with (right) chemical anchoring. (b) Adhesive and cohesive failures of the LMC sample (ϕ_{LM} = 20%, droplet size (d) = 2 μm) in T-peel without and with APTES surface treatment. (c) Fracture energies of the LMCs in T-peel. Reprinted from Ref. [28].

of high-performance e-skins leveraging LMCs with enhanced adhesion and fracture energy underscores their potential for diverse applications in soft electronics, particularly in the medical and biomedical fields.

In addition, many substrate materials, including paper and textiles, exhibit weak adhesion to LMs, limiting their application to diverse substrates.

Wu *et al.* [81] introduced a convenient and cost-effective method for preparing printable LM microgel (LMM) inks by encapsulating LM microdroplets with alginate microgel shells. This approach addresses the challenges related to the high surface tension and strong fluidity of LMs, which hinder their ability to form precise patterns with a high resolution. The process began with the addition of LM to a sodium alginate solution, followed by mechanical stirring to achieve a homogeneous dispersion of LM droplets. Subsequently, centrifugation separated the lightweight mixture of the sodium alginate solution, resulting in a concentrated LMM ink composed of LM microdroplets encapsulated by alginate microgel shells. The breakup of large LM volumes into fine droplets during this process leads to the formation of microgel shells on the surface of the LM microdroplets. During the initial stages of the 3D processing of the LMM ink, hydrogen-bonding networks formed, leading to a reduction in its fluidity. These hydrogen bonds are held together by physical forces and can be disrupted by shear forces. During extrusion, the hydrogen-bonding network was broken by shear forces, which reduced the viscosity of the composite. Once the shear forces dissipated, the hydrogen-bonding network was reestablished to maintain the desired printing form. The encapsulation of LM microdroplets with alginate microgel shells enables the preparation of LMM inks that are suitable for printing applications. This method overcomes the challenges related to fluidity, substrate adhesion, and patterning resolution, and offers a promising avenue for the development of functional electronic devices, particularly in flexible electronics and biomedical applications.

Ding *et al.* [29] developed a novel method for adhering composites to the human skin, specifically focusing on adhesive LMPs (ALMPs) that can be deposited directly onto the skin *in situ*. ALMPs exhibit excellent skin contact impedance, biocompatibility, and permeability, making them suitable for permanent use on the skin. Oxygen from the oxide layer formed hydroxyl groups on the polymer chains, resulting in the creation of hydrogen bonds. The outermost layer of polyvinyl alcohol (PVA) interacts with keratin on the epidermis, forming a strong adhesion between the ALMP and the skin. The ALMP produced via *in situ* deposition demonstrated abrasion resistance by withstanding up to 1600 cm of loaded paper tape wear and handling up to 175 g of tape, thus proving their durability.

ALMPs exhibit skin-adhesive properties with ultralow skin contact impedance and high-quality conductivity. The ALMP conformed to the skin upon initial contact without leaving any gaps (Fig. 14(a)). In contrast, the film-type LM adheres to the skin but cannot directly contact it, leaving gaps in the epidermis (Fig. 14(b)). Adhesive-type LM electrodes can indirectly contact the epidermis with the assistance of

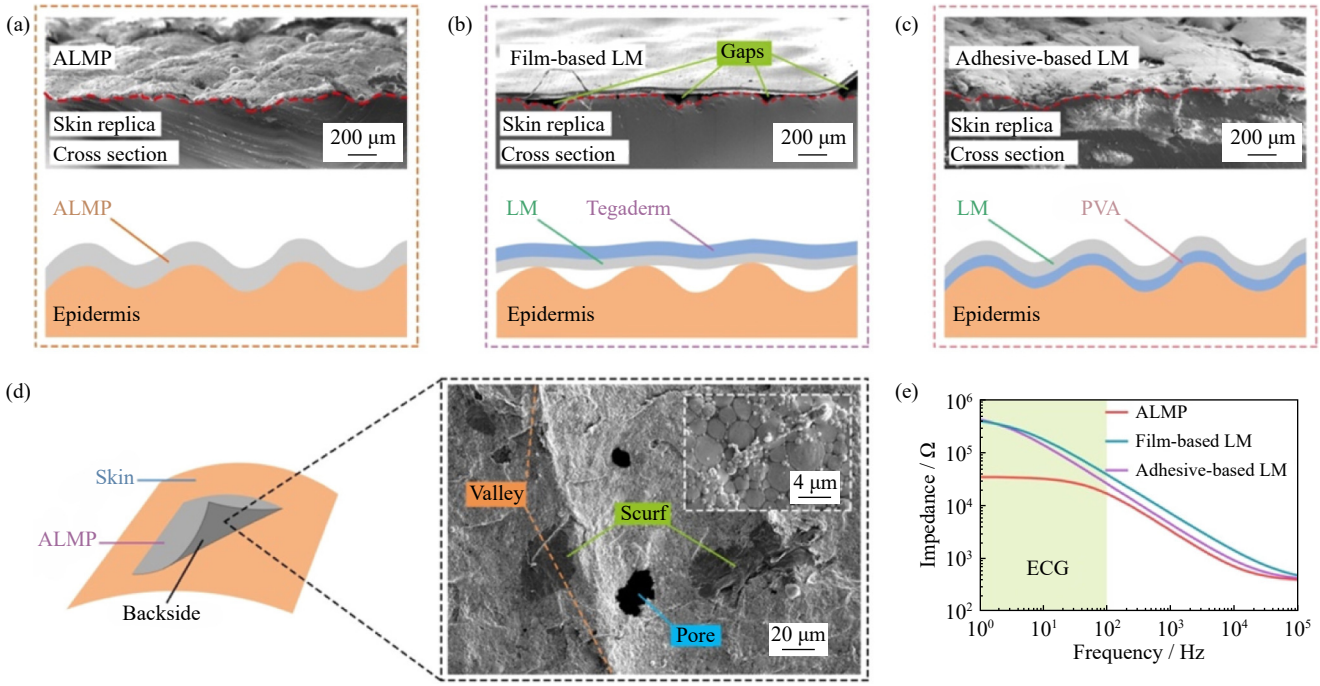


Fig. 14. Skin adhesion and ultraconformality result in a better electrophysiologic signal. (a) SEM picture of the ALMP on the skin replica. (b) SEM picture of the film-based LM electrode on the skin replica. (c) SEM picture of the adhesive-based LM electrode on the skin replica. (d) SEM picture of the face of the ALMP coating contacting the skin. The "valley" corresponds to the fold of the skin. The "pore" corresponds to the sweat-wicking pore of the skin. The "scurf" on the ALMP shows that the ALMP coating is tightly bound to the skin. (e) Skin contact impedances of the three electrodes. ECG refers to electrocardiogram. Reprinted with permission from L. Ding, C. Hang, S.J. Yang, *et al.*, *Nano Lett.*, vol. 22, 4482-4490 (2022) [29]. Copyright 2022 American Chemical Society.

PVA (Fig. 14(c)). The texture on the back of the ALMP closely resembled that of the human skin (Fig. 14(d)). Owing to gravitational flattening, particles can firmly contact the human skin. Experimental results comparing the skin contact impedances among the three electrodes confirmed that the ALMP has a relatively lower skin contact impedance compared to other types of electrodes (Fig. 14(e)). In conclusion, ALMP-based epidermal electronics have the potential for precise health monitoring and disease diagnosis.

An e-skin made with an LM can also be integrated with energy harvesting technologies. Among the various energy harvesting methods, a triboelectric nanogenerator (TENG) converts mechanical energy into electrical energy by utilizing the triboelectric effect and electrostatic induction. Electricity is generated through a separation mechanism driven by the intrinsic tendency of transfer of surface electrons when two different materials come into contact and then separate [84–85]. A TENG can utilize biomechanical motion from the body to produce electrical energy, making it highly applicable for e-skins and sensors. To be effective, TENGs must possess environmentally friendly characteristics, high power density, flexibility, and lightweight properties [86–88]. LM, with its low toxicity, environmental friendliness, and excellent stretchability, is a suitable candidate for use in TENGs. However, the oxide layer that forms on the surface of the LM can alter its properties, highlighting the need for research into methods to effectively control this factor.

Yang *et al.* [89] developed a stretchable energy-harvesting e-skin utilizing LM. This tactile interface, based on a TENG, features a Galinstan liquid metal nanoparticle (LM-NP) film as a stretchable electrode and a patterned PDMS layer serving dual functions as a friction layer and an encapsulation material. The resulting e-skin demonstrated exceptional properties, including a high stretchability of approximately 260% and an impressive sensitivity of 2.52 $V \cdot kPa^{-1}$. Moreover, it exhibited stable and reliable output performance and pressure-sensing capabilities under various tensile conditions. By developing a high-performance energy-harvesting e-skin using a simple and cost-effective approach, the team has demonstrated its potential for applications in diverse fields, such as soft robotics and flexible electronic devices.

5. Challenges and conclusion

LMCs are materials that combine alloys of Ga, In, Sn, and other metals with solid particles, fibers, or other substances. They possess unique properties, such as high electrical conductivity, high thermal conductivity, and good mechanical strength, making them suitable for a wide range of applications, including heat exchangers, electronic devices, and biomedical implants. However, several areas of LMCs need to be addressed and researched. First, LMCs are challenging to manufacture because of the low viscosity of LMs and the tendency of solid particles to aggregate. Research is needed to develop new processing technologies that can produce LMCs with uniform dispersion and distribution of solid particles. In addition, LMCs are prone to oxidation and corrosion, which can affect their performance and durability. To address these issues, researchers are exploring methods to enhance the stability of LMCs by adding protective coatings or modifying their alloy compositions. The mechanical properties of LMCs are influenced by the type, size, and volume fraction of solid particles. Further research is required to optimize the particle size and volume fraction to improve the mechanical strength of LMCs. Studies on the cytotoxicity of LMCs are limited. Further research is required to establish their biocompatibility for commercial applications. Demonstrating biocompatibility through further research is essential to obtaining approval for biomedical applications. Additionally, incorporating advanced technologies such as artificial intelligence and numerical simulation could accelerate the discovery and optimization of LMCs with novel properties. The development of LM gradient composites may unlock new applications in chips, quantum devices, and energy generation. Table 1 summarizes the key properties, fabrication methods, and potential applications of different types of LMCs, highlighting the advantages and challenges associ-

Table 1. LMCs: Properties, fabrication methods, and applications

Type of liquid-metal composite	Advantages	Fabrication methods	Application	Challenges
Liquid metal core–shell composites	Enhanced stability: The core–shell structure provides mechanical and chemical stability. Property integration: Combines properties of core and shell materials.	Surface oxidation; ligand assembly; galvanic replacement	Electromagnetic interference (EMI) shielding; conductive inks	Manufacturing complexity; oxidation and corrosion; particle dispersion; biocompatibility concerns
Liquid metal–polymer composites	Retention of polymer properties: Preserves the flexibility and elasticity of polymers. Added conductivity: Introduces high electrical and thermal conductivity from liquid metal.	Planetary mixing; overhead mixing; sonication	Soft actuators and sensors; electronic skins	
Liquid metal–particle composites	Property enhancement: Enhances liquid metal properties (e.g., thermal conductivity). Tunable characteristics: Adjustable properties with various additives.		Thermal interface materials; flexible electronics; printed electronics	

ated with each composite. This overview provides a clear understanding of where current research efforts should be focused to overcome the existing challenges in this field. In summary, while LMCs offer promising characteristics, ongoing research is crucial for addressing manufacturing challenges, enhancing stability, optimizing mechanical properties, and establishing biocompatibility for broader applications in various industries. Although existing challenges still remain, the rapid development of LMCs in recent years has indicated a bright future for this new generation of functional materials. Future research should focus on enhancing material interfaces, improving stability, and advancing computational methods for efficient design and optimization to realize their full potential. Additionally, integrating sustainability by incorporating renewable or recyclable components can open new pathways for eco-friendly applications. With sustained efforts, LMCs can potentially enable considerable advancements in soft robotics, energy storage, and biomedicine, marking them as key materials for next-generation technologies.

Acknowledgements

This research was supported by the GRDC (Global Research Development Center) Cooperative Hub Program through the National Research Foundation of Korea (NRF), funded by the Ministry of Science and ICT (MSIT) (No. RS-2023-00257595).

Conflict of Interest

The authors declare no conflict of interest.

Open Access Funding enabled and organized by Chung-Ang University.

Open Access This article is licensed under a Creative Commons Attribution 4.0 International License, which permits use, sharing, adaptation, distribution and reproduction in any medium or format, as long as you give appropriate credit to the original author(s) and the source, provide a link to the Creative Commons license, and indicate if changes were made. The images or other third party material in this article are included in the article's Creative Commons licensee, unless indicated otherwise in a credit line to the material. If material is not included in the article's Creative Commons license and your intended use is not permitted by statutory regulation or exceeds the permitted use, you will need to obtain permission directly from the copyright holder. To view a copy of this license, visit http://creativecommons.org/licenses/ by/4.0/.

References

[1] R.W. Style, R. Tutika, J.Y. Kim, and M.D. Bartlett, Solid–liquid composites for soft multifunctional materials, *Adv. Funct. Mater.*, 31(2021), No. 1, art. No. 2005804.

[2] H. Li, R. Qiao, T.P. Davis, and S.Y. Tang, Biomedical applications of liquid metal nanoparticles: A critical review, *Biosensors*, 10(2020), No. 12, art. No. 196.

[3] M.G. Nicholas and C.F. Old, Liquid metal embrittlement, *J. Mater. Sci.*, 14(1979), No. 1, p. 1.

[4] Q. Wang, Y. Yu, and J. Liu, Preparations, characteristics and applications of the functional liquid metal materials, *Adv. Eng. Mater.*, 20(2018), No. 5, art. No. 1700781.

[5] K.N. Paracha, A.D. Butt, A.S. Alghamdi, S.A. Babale, and P.J. Soh, Liquid metal antennas: Materials, fabrication and applications, *Sensors*, 20(2019), No. 1, art. No. 177.

[6] B. Hwang, Y. Han, and P. Matteini, Bending fatigue behavior of Ag nanowire/Cu thin-film hybrid interconnects for wearable electronics, *Facta Univ. Ser. Mech. Eng.*, 20(2022), No. 3, p. 553.

[7] H. Kim, G. Kim, J.H. Kang, M.J. Oh, N. Qaiser, and B. Hwang, Intrinsically conductive and highly stretchable liquid metal/carbon nanotube/elastomer composites for strain sensing and electromagnetic wave absorption, *Adv. Compos. Hybrid Mater.*, 8(2025), art. No. 14.

[8] K.B. Ozutemiz, J. Wissman, O.B. Ozdoganlar, and C. Majidi, EGaIn–metal interfacing for liquid metal circuitry and microelectronics integration, *Adv. Mater. Interfaces*, 5(2018), No. 10, art. No. 1701596.

[9] G.J. Hayes, J.H. So, A. Qusba, M.D. Dickey, and G. Lazzi, Flexible liquid metal alloy (EGaIn) microstrip patch antenna, *IEEE Trans. Anntenas. Propag.*, 60(2012), No. 5, p. 2151.

[10] M.D. Dickey, Stretchable and soft electronics using liquid metals, *Adv. Mater.*, 29(2017), No. 27, art. No. 1606425.

[11] L. Battezzati and A.L. Greer, The viscosity of liquid metals and alloys, *Acta Metall.*, 37(1989), No. 7, p. 1791.

[12] B. Giordanengo, N. Benazzi, J. Vinckel, J.G. Gasser, and L. Roubi, Thermal conductivity of liquid metals and metallic alloys, *J. Non Cryst. Solids*, 250(1999), p. 377.

[13] G.Y. Bo, L. Ren, X. Xu, Y. Du, and S.X. Dou, Recent progress on liquid metals and their applications, *Adv. Phys. X*, 3(2018), No. 1, art. No. 1446359.

[14] J. V. Naidich, The wettability of solids by liquid metals, [in] D.A. Cadenhead and J.F. Danielli, eds., *Progress in Surface and Membrane Science*, Vol. 14, Academic Press, New York, 1981, p. 353.

[15] J.H. Kim, S. Kim, J.H. So, K. Kim, and H.J. Koo, Cytotoxicity of gallium–indium liquid metal in an aqueous environment, *ACS Appl. Mater. Interfaces*, 10(2018), No. 20, p. 17448.

[16] R. Tutika, S.H. Zhou, R.E. Napolitano, and M.D. Bartlett, Mechanical and functional tradeoffs in multiphase liquid metal, solid particle soft composites, *Adv. Funct. Mater.*, 28(2018), No. 45, art. No. 1804336.

[17] M.J. Ford, D.K. Patel, C. Pan, S. Bergbreiter, and C. Majidi, Controlled assembly of liquid metal inclusions as a general approach for multifunctional composites, *Adv Mater*, 32(2020), No. 46, art. No. 2002929.

[18] H. Ha, N. Qaiser, T.G. Yun, J.Y. Cheong, S. Lim, and B. Hwang, Sensing mechanism and application of mechanical strain sensor: A mini-review, *Facta Univ. Ser. Mech. Eng.*, 21(2023), No. 4, p. 751.

[19] N. Kazem, T. Hellebrekers, and C. Majidi, Soft multifunctional composites and emulsions with liquid metals, *Adv. Mater.*, 29(2017), No. 27, art. No. 1605985.

[20] H. Kim, N. Qaiser, and B. Hwang, Electro-mechanical response of stretchable PDMS composites with a hybrid filler system, *Facta Univ. Ser. Mech. Eng.*, 21(2023), No. 1, p. 051.

[21] C. Chiew and M.H. Malakooti, A double inclusion model for liquid metal polymer composites, *Compos. Sci. Technol.*, 208(2021), art. No. 108752.

[22] M.D. Bartlett, N. Kazem, M.J. Powell-Palm, *et al.*, High thermal conductivity in soft elastomers with elongated liquid metal inclusions, *Proc. Natl. Acad. Sci. U.S.A.*, 114(2017), No. 9, p. 2143.

[23] J. Diani, B. Fayolle, and P. Gilormini, A review on the Mullins effect, *Eur. Polym. J.*, 45(2009), No. 3, p. 601.
[24] X.L. Wang, W.H. Yao, R. Guo, *et al*., Soft and moldable Mg-doped liquid metal for conformable skin tumor photothermal therapy, *Adv. Healthcare Mater.*, 7(2018), No. 14, art. No. 1800318.
[25] R. Tutika, A.B.M.T. Haque, and M.D. Bartlett, Self-healing liquid metal composite for reconfigurable and recyclable soft electronics, *Commun. Mater.*, 2(2021), art. No. 64.
[26] Y. Li, Y.G. Cui, M.J. Zhang, *et al*., Ultrasensitive pressure sensor sponge using liquid metal modulated nitrogen-doped graphene nanosheets, *Nano Lett.*, 22(2022), No. 7, p. 2817.
[27] J.Y. Yang, K.Y. Kwon, S. Kanetkar, *et al*., Skin-inspired capacitive stress sensor with large dynamic range via bilayer liquid metal elastomers, *Adv. Mater. Technol.*, 7(2022), No. 5, art. No. 2101074.
[28] T.A. Pozarycki, D. Hwang, E.J. Barron III, B.T. Wilcox, R. Tutika, and M.D. Bartlett, Tough bonding of liquid metal-elastomer composites for multifunctional adhesives, *Small*, 18(2022), No. 41, art. No. 2203700.
[29] L. Ding, C. Hang, S.J. Yang, *et al.*, *In situ* deposition of skin-adhesive liquid metal particles with robust wear resistance for epidermal electronics, *Nano Lett.*, 22(2022), No. 11, p. 4482.
[30] R. Tutika, S. Kmiec, A.B.M.T. Haque, S.W. Martin, and M.D. Bartlett, Liquid metal–elastomer soft composites with independently controllable and highly tunable droplet size and volume loading, *ACS Appl. Mater. Interfaces*, 11(2019), No. 19, art. No. 17873.
[31] M. Zadan, M.H. Malakooti, and C. Majidi, Soft and stretchable thermoelectric generators enabled by liquid metal elastomer composites, *ACS Appl. Mater. Interfaces*, 12(2020), No. 15, p. 17921.
[32] H. Ha, S. Müller, R.P. Baumann, and B. Hwang, Peakforce quantitative nanomechanical mapping for surface energy characterization on the nanoscale: A mini-review, *Facta Univ. Ser. Mech. Eng.*, 22(2024), No. 1, p. 001.
[33] D. Amoabeng and S.S. Velankar, A review of conductive polymer composites filled with low melting point metal alloys, *Polym. Eng. Sci.*, 58(2018), No. 6, p. 1010.
[34] S. Zhu, J.H. So, R. Mays, *et al*., Ultrastretchable fibers with metallic conductivity using a liquid metal alloy core, *Adv. Funct. Mater.*, 23(2013), No. 18, p. 2308.
[35] F. Delannay, L. Froyen, and A. Deruyttere, The wetting of solids by molten metals and its relation to the preparation of metal-matrix composites composites, *J. Mater. Sci.*, 22(1987), No. 1, p. 1.
[36] J. Kaczmar, K. Pietrzak and W. Włosiński, The production and application of metal matrix composite materials, *J. Mater. Process. Technol.*, 106(2000), No. 1-3, p. 58.
[37] G.G. Guymon and M.H. Malakooti, Multifunctional liquid metal polymer composites, *J. Polym. Sci.*, 60(2022), No. 8, p. 1300.
[38] C.P. Ambulo, M.J. Ford, K. Searles, C. Majidi, and T.H. Ware, 4D-printable liquid metal–liquid crystal elastomer composites, *ACS Appl Mater Interfaces*, 13(2021), No. 11, p. 12805.
[39] A.B.M.T. Haque, R. Tutika, R.L. Byrum, and M.D. Bartlett, Programmable liquid metal microstructures for multifunctional soft thermal composites, *Adv. Funct. Mater.*, 30(2020), No. 25, art. No. 2000832.
[40] M.G. Saborio, S.X. Cai, J.B. Tang, *et al*., Liquid metal droplet and graphene co-fillers for electrically conductive flexible composites, *Small*, 16(2020), No. 12, art. No. 1903753.
[41] X. Qian, J.W. Zhou, and G. Chen, Phonon-engineered extreme thermal conductivity materials, *Nat. Mater.*, 20(2021), No. 9, p. 1188.
[42] H.A. Eivari, Z. Sohbatzadeh, P. Mele, and M.H.N. Assadi, Low thermal conductivity: Fundamentals and theoretical aspects in thermoelectric applications, *Mater. Today Energy*, 21(2021), art. No. 100744.
[43] E.C. Onyibo and M. Asmael, State-of-the-art review of springback behavior of polymers, *Spectr. Mech. Eng. Oper. Res.*, 1(2024), No. 1, p. 272.
[44] W. Zeng, X.M. Tao, S.P. Lin, *et al*., Defect-engineered reduced graphene oxide sheets with high electric conductivity and controlled thermal conductivity for soft and flexible wearable thermoelectric generators, *Nano Energy*, 54(2018), p. 163.
[45] M. Jonson and G.D. Mahan, Mott's formula for the thermopower and the Wiedemann-Franz law, *Phys. Rev. B*, 21(1980), No. 10, p. 4223.
[46] L.M. Tan, J.B. Zhang, and J. Shen, Liquid metal/metal porous skeleton with high thermal conductivity and stable thermal reliability, *J. Mater. Sci.*, 58(2023), No. 47, p. 17829.
[47] S. Kim, J. Park, Y.H. Pi, *et al*., Facile low-oxidation emulsification of liquid metal using polyvinylpyrrolidone for highly viscoelastic heat conductive pastes, *ACS Appl. Eng. Mater.*, 2(2024), No. 11, p. 2705.
[48] S.L. Wang and S.A. Chester, Modeling thermal recovery of the Mullins effect, *Mech. Mater.*, 126(2018), p. 88.
[49] S.Y. Tang and R.R. Qiao, Liquid metal particles and polymers: A soft–soft system with exciting properties, *Acc. Mater. Res.*, 2(2021), No. 10, p. 966.
[50] P.S. Banerjee, D.K. Rana, and S.S. Banerjee, Influence of microstructural alterations of liquid metal and its interfacial interactions with rubber on multifunctional properties of soft composite materials, *Adv. Colloid Interface Sci.*, 308(2022), art. No. 102752.
[51] T.S. Munonde and P.N. Nomngongo, Nanocomposites for electrochemical sensors and their applications on the detection of trace metals in environmental water samples, *Sensors*, 21(2021), No. 1, art. No. 131.
[52] I. Zaied, H. Fitouri, Z. Chine, A. Rebey, and B. El Jani, Atmospheric-pressure metal–organic vapor-phase epitaxy of GaAsBi alloys on high-index GaAs substrates, *J. Phys. Chem. Solids*, 75(2014), No. 2, p. 244.
[53] H.G. Chen, Z.C. Guo, H.S. Wang, W.Y. Huang, F. Pan, and Z.Q. Wang, A liquid metal interlayer for boosted charge transfer and dendrite-free deposition toward high-performance Zn anodes, *Energy Storage Mater.*, 54(2023), p. 563.
[54] Y. Liu, W. Zhang, and H. Wang, Synthesis and application of core–shell liquid metal particles: A perspective of surface engineering, *Mater. Horiz.*, 8(2021), No. 1, p. 56.
[55] Z. Li, Y.M. Guo, Y.F. Zong, *et al*., Ga based particles, alloys and composites: Fabrication and applications, *Nanomaterials*, 11(2021), No. 9, art. No. 2246.
[56] C. Chiew, M.J. Morris, and M.H. Malakooti, Functional liquid metal nanoparticles: Synthesis and applications, *Mater. Adv.*, 2(2021), No. 24, p. 7799.
[57] T. Daeneke, K. Khoshmanesh, N. Mahmood, *et al*., Liquid metals: Fundamentals and applications in chemistry, *Chem. Soc. Rev.*, 47(2018), No. 11, p. 4073.
[58] C. Choi, N. Qaiser, and B. Hwang, Mechanically pressed polymer-matrix composites with 3D structured filler networks for electromagnetic interference shielding application, *Facta Univ. Ser. Mech. Eng.*, 22(2024), No. 4, p. 601.
[59] S. Chen, H.Z. Wang, R.Q. Zhao, W. Rao, and J. Liu, Liquid metal composites, *Matter*, 2(2020), No. 6, p. 1446.
[60] M.J. Regan, H. Tostmann, P.S. Pershan, *et al*., X-ray study of the oxidation of liquid-gallium surfaces, *Phys. Rev. B*, 55(1997), No. 16, p. 10786.
[61] A.J. Downs, *Chemistry of Aluminium, Gallium, Indium and Thallium*, Springer Dordrecht, New York, 1993.
[62] M.D. Dickey, Emerging applications of liquid metals featuring surface oxides, *ACS Appl. Mater. Interfaces*, 6(2014), No. 21, p. 18369.
[63] L. Mou, J. Qi, L.X. Tang, *et al*., Highly stretchable and biocom-

patible liquid metal-elastomer conductors for self-healing electronics, *Small*, 16(2020), No. 51, art. No. 2005336.
[64] M.A. Rahim, F. Centurion, J.L. Han, *et al*., Polyphenol-induced adhesive liquid metal inks for substrate-independent direct pen writing, *Adv. Funct. Mater.*, 31(2021), No. 10, art. No. 2007336.
[65] H. Wang, W.K. Xing, S. Chen, C.Y. Song, M.D. Dickey, and T. Deng, Liquid metal composites with enhanced thermal conductivity and stability using molecular thermal linker, *Adv. Mater.*, 33(2021), No. 43, art. No. 2103104.
[66] H. Wang, Y. Yao, Z. He, *et al*., A highly stretchable liquid metal polymer as reversible transitional insulator and conductor, *Adv Mater*, 31(2019), No. 23, art. No. 1901337.
[67] B. Chen, Y. Cao, Q. Li, *et al*., Liquid metal-tailored gluten network for protein-based e-skin, *Nat. Commun.*, 13(2022), No. 1, art. No. 1206.
[68] W. Babatain, M.S. Kim, and M.M. Hussain, From droplets to devices: Recent advances in liquid metal droplet enabled electronics, *Adv. Funct. Mater.*, 34(2024), No. 31, art. No. 2308116.
[69] Y.F. Wang, M. Mayyas, J. Yang, *et al*., Self-deposition of 2D molybdenum sulfides on liquid metals, *Adv. Funct. Mater.*, 31(2021), No. 3, art. No. 2005866.
[70] Y.L. Lin, J. Genzer, and M.D. Dickey, Attributes, fabrication, and applications of gallium-based liquid metal particles, *Adv. Sci.*, 7(2020), No. 12, art. No. 2000192.
[71] B. Zhao, Y.Q. Du, H.L. Lv, *et al*., Liquid-metal-assisted programmed galvanic engineering of core–shell nanohybrids for microwave absorption, *Adv. Funct. Mater.*, 33(2023), No. 34, art. No. 2302172.
[72] R.M. Zheng, Z.F. Peng, Y. Fu, *et al*., A novel conductive core–shell particle based on liquid metal for fabricating real-time self-repairing flexible circuits, *Adv. Funct. Mater.*, 30(2020), No. 15, art. No. 1910524.
[73] Y. Wang, Y.N. Gao, T.N. Yue, X.D. Chen, R.C. Che, and M. Wang, Liquid metal coated copper micro-particles to construct core-shell structure and multiple heterojunctions for high-efficiency microwave absorption, *J. Colloid Interface Sci.*, 607(2022), p. 210.
[74] J. Ma, Y. Lin, Y.W. Kim, *et al*., Liquid metal nanoparticles as initiators for radical polymerization of vinyl monomers, *ACS Macro Lett.*, 8(2019), No. 11, p. 1522.
[75] J.W. Boley, E.L. White, and R.K. Kramer, Mechanically sintered gallium–indium nanoparticles, *Adv Mater*, 27(2015), No. 14, p. 2355.
[76] A. Hajalilou, A.F. Silva, P.A. Lopes, E. Parvini, C. Majidi, and M. Tavakoli, Biphasic liquid metal composites for sinter-free printed stretchable electronics, *Adv. Mater. Interfaces*, 9(2022), No. 5, art. No. 2101913.
[77] X.T. Xue, D.G. Zhang, Y.L. Wu, *et al*., Segregated and non-settling liquid metal elastomer via jamming of elastomeric particles, *Adv. Funct. Mater.*, 33(2023), No. 6, art. No. 2210553.
[78] M.K. Zhang, S.Y. Yao, W. Rao, and J. Liu, Transformable soft liquid metal micro/nanomaterials, *Mater. Sci. Eng. R*, 138(2019), p. 1.
[79] S. Liu, M.C. Yuen, E.L. White, *et al*., Laser sintering of liquid metal nanoparticles for scalable manufacturing of soft and flexible electronics, *ACS Appl. Mater. Interfaces*, 10(2018), No. 33, p. 28232.
[80] N. Kazem, M.D. Bartlett, and C. Majidi, Extreme toughening of soft materials with liquid metal, *Adv. Mater.*, 30(2018), No. 22, art. No. 1706594.
[81] P. Wu, J. Fu, Y. Xu, and Y. He, Liquid metal microgels for three-dimensional printing of smart electronic clothes, *ACS Appl Mater Interfaces*, 14(2022), No. 11, p. 13458.
[82] W. Kong, Z. Wang, M. Wang, *et al.*, Oxide-mediated formation of chemically stable tungsten–liquid metal mixtures for enhanced thermal interfaces, *Adv. Mater.*, 31(2019), No. 44, art. No. 1904309.
[83] X.K. He, J.P. Wu, S.H. Xuan, S.S. Sun, and X.L. Gong, Stretchable and recyclable liquid metal droplets embedded elastomer composite with high mechanically sensitive conductivity, *ACS Appl. Mater. Interfaces*, 14(2022), No. 7, p. 9597.
[84] H. Zou, Y. Zhang, L. Guo, *et al*., Quantifying the triboelectric series, *Nat. Commun.*, 10(2019), No. 1, art. No. 1427.
[85] L.L. Zhou, D. Liu, J. Wang, and Z.L. Wang, Triboelectric nanogenerators: Fundamental physics and potential applications, *Friction*, 8(2020), No. 3, p. 481.
[86] X. Pu, C. Zhang, and Z.L. Wang, Triboelectric nanogenerators as wearable power sources and self-powered sensors, *Natl. Sci. Rev.*, 10(2022), No. 1, art. No. nwac170.
[87] B. Nowacki, K. Mistewicz, S. Hajra, and H.J. Kim, 3D printed triboelectric nanogenerator for underwater ultrasonic sensing, *Ultrasonics*, 133(2023), art. No. 107045.
[88] Z.T. Wei, J.L. Wang, Y.H. Liu, *et al*., Sustainable triboelectric materials for smart active sensing systems, *Adv. Funct. Mater.*, 32(2022), No. 52, art. No. 2208277.
[89] Y.J. Yang, J. Han, J.R. Huang, *et al*., Stretchable energy-harvesting tactile interactive interface with liquid-metal-nanoparticle-based electrodes, *Adv. Funct. Mater.*, 30(2020), No. 29, art. No. 1909652.